Journal Name

ARTICLE

Evaluation of *in vitro* wound adhesion characteristics of composite film and wafer based dressings using texture analysis and FTIR spectroscopy: A chemometrics factor analysis approach.

J. S. Boateng[*a], H. V. Pawar [a], and J. Tetteh[a]

[a] Department of Pharmaceutical, Chemical and Environmental Sciences, Faculty of Engineering and Science, University of Greenwich at Medway, Chatham Maritime, Kent, UK, ME4 4TB

*Corresponding author:
Dr Joshua Boateng
Email: j.s.boateng@gre.ac.uk; joshboat40@gmail.com
Tel: +44 (0) 208 331 8980

Abstract

The adhesive properties of two dressing types, solvent cast films and freeze-dried wafers have been determined and compared using two analytical techniques, combined with chemometrics data analysis. Films and wafers were prepared from gels containing polyox (POL) combined with carrageenan (CAR) or sodium alginate (SA), glycerol (GLY) as plasticiser (films) with streptomycin and diclofenac as model drugs. The gels were dried in an oven at 40°C or freeze-dried to obtain films and wafers respectively. The adhesive performance of the films and wafers was assessed with 6.67% w/v gel using a texture analyser to measure the stickiness, work of adhesion and cohesiveness. The effect of viscosity of simulated wound fluid[(containing (2% w/w or 5% w/w bovine serum albumin)] and mucin solution (2% w/w) present on the gelatin surface on texture analyser profiles was investigated. Furthermore, the adhesive properties were estimated and evaluated using attenuated total reflectance Fourier transform infrared spectroscopy by monitoring the diffusion of mucin solution [2% w/w in phosphate buffered saline (PBS) pH 7.4] through the formulations. The diffusion data was analysed using target factor analysis (chemometrics approach) to establish proof of concept for predicting adhesion by measuring mucin interaction and its diffusion through films and wafers. There was a significant effect of simulated wound fluid, viscosity, plasticizer (for films) and drug loading on the adhesive performance of both films and wafers. POL-SA films showed higher mucoadhesive performance in the presence of viscous simulated wound fluid containing 5% bovine serum albumin. Wafers and plasticised films demonstrated high detachment force indicating strong interactions between the chains of the polymers (POL, SA and CAR) and the model wound surface (gelatin). ATR-FTIR spectroscopy showed that mucin diffused independently through the solvent and across the films and wafers. POL-CAR films generally showed slower diffusion of mucin when compared with POL-SA films whilst the opposite effect was observed for diffusion through POL-CAR wafers and POL-SA wafers. Generally, diffusion through wafers was faster than the corresponding films.

1. Introduction

Dressings are required to exhibit certain functional properties such as stress resistance, softness, flexibility, pliability, elasticity and bioadhesion which provide valuable information on key performance characteristics that are deemed essential for wound healing applications[1]. The development of prolonged and/or controlled release mucosal formulations (including medicated wound dressings) has often utilized bioadhesive polymers which can adhere to the cellular

secretions, mucus, extracellular matrix, cells or tissues in the presence of water or wound exudate[2-4]. Such dressings include freeze-dried wafers and the more established flexible films obtained by solvent casting. Though the solvent casting approach is simple and allows ease of production of free and flexible films, the process is not easily versatile and does not lend itself to easy scale up and manufacturing on a large scale. Recently, electrospinning has gained increased interest in various fields. Electrospinning involves the use of an electric field to spin fibres with sub-micron diameters (e.g. nanofibers). In this process, a electrospinning single or co-axial multi-needle is used to direct an electrified liquid formulation jet towards a ground electrode during which time solvent can be evaporated, forming solid nanofibers[5]. The main advantages include single step process, use of ambient conditions, low cost and no need for high concentrations of additives or surfactants[6]. Electrospinned fibres have been used in various applications including wound dressings and drug delivery systems. For example, new gyratory methods where smart molecules can be tagged onto the fibres have potential use in formulation of therapeutic dressings which can take active part in the wound healing process, therefore enhancing tissue regeneration. Zhang and co-workers[7] employed an infusion gyration approach to develop biohybrid nanofibres comprising functionalised biomaterials integrated with active proteins with intelligent properties which have great potential for tissue regeneration applications including wound healing.

In the case of wounds, prolonged residence time of the dressing is an essential functionality since frequent dressing changes, which also causes pain, is a major source of patient non-compliance, and can result in complications and delays in wound healing[8-9].

It has been suggested that the interaction between a mucosal (moist) surface and mucoadhesive polymers is a result of physical entanglement and secondary interactive forces, mainly due to hydrogen bonding and van der Waals attraction forces which depend upon the chemical structure of the polymer[10]. Peppas and Buri proposed certain characteristics which are necessary for effective mucoadhesion. These include polymers containing strong H-bonding groups, strong anionic charges, high molecular weight, sufficient chain flexibility, and surface energy properties which favour spreading of the polymer onto the mucosal surface[11]. For the purpose of wound dressings, adhesive properties of the polymers could be affected by degree of hydration, amount of exudate released from the wound, exudate viscosity, salts and proteins present in exudate, presence of microorganisms as well as the depth and area of the wound[12].

There are different approaches used to evaluate the adhesive performance of polymers and polymeric dosage forms. These include texture analyser[9-10, 13-15], rheometric measurements[16] and attenuated total reflection-Fourier transform infrared

(ATR-FTIR) spectroscopy[2, 17]. Recently, texture analyser has been used for studying properties of mucoadhesive polymers and dosage forms using tensile mode of testing. These *in vitro* experiments involve attaching the dosage form to a probe and force applied to bring the sample in contact with a representative mucosal substrate for a specific time (contact time) and a mechanical force applied to detach the probe from the mucosal substrate[3, 18]. The adhesive strength (stickiness) is evaluated by the force (F_{max}) required to detach the sample from the model mucosal substrate after mucoadhesive bonding has been established[19]. Total work of adhesion represents the total amount of energy involved in the withdrawal of the probe from the mucosal surface and determined by the area under the force versus distance curve. Cohesiveness determines the ability of the sample to resist the separation from the mucosal (wound) substrate due to the intermolecular forces (such as those from hydrogen bonding and van der Waals forces). It is determined through the distance travelled by sample before being detached[10, 20-22].

Mucoadhesion by means of a texture analyser usually involves the measurement of mechanical force required to fracture the interface between a substrate or mucin and polymer and therefore depends largely upon the fracture theory of mucoadhesion[17]. Saiano and co-workers[2] reported that variations in the experimental parameters such as contact time, contact force, test speed and rate of removal from the adhesive test surface consequently results in variations in experimental muco-(bio)-adhesive results. Such variations make it very difficult to compare data from different investigators to assign exact values representing bioadhesive / mucoadhesive performance[2]. Further, Jabbari and co-workers reported that though mucoadhesion studies using a texture analyser is advantageous for classification of mucoadhesive polymers, it is not an accurate technique for determining mechanisms of adhesion at the biointerface[17]. As a result, alternative spectroscopic analysis techniques have been implemented and adopted to investigate the interaction between substrates and the polymer matrix to help evaluate mucoadhesion mechanisms. In particular, ATR–FTIR has been applied effectively to study the interpenetration and entanglement of polymer chains and mucous which is fundamentally based on the diffusion theory of mucoadhesion[2, 17]. ATR–FTIR can also be used to study mucoadhesion properties and diffusion profiles of solvent through different membrane surfaces such as biological tissues, films and silicon membranes[2, 23] since it can provide real time information of diffusion of materials such as mucin through the membranes.

However, measurement of kinetic diffusion of mucin solution across the polymer based on FTIR spectroscopy generally produces large quantities of often complex multivariate data sets that require appropriate chemometric analysis. The employment of chemometric techniques generally involves

calibration, validation and extraction of maximum chemical information from the analytical data and its usefulness has previously been reviewed[24]. Among the chemometric techniques used to resolve complex spectral data, factor analysis or principal component analysis[25-26] based on singular value decomposition are the most common. Factor analysis is a multivariate technique for reduction of data matrices into its lowest dimensionality by the use of orthogonal factor space and transformation that yields predictions and/or recognisable factors which influence the data matrix.

In this paper, we report on the *in vitro* wound adhesion properties of two different dressing formulations (films and wafers) both comprising two different polymers (composite) and two drugs, using texture analysis and ATR-FTIR spectroscopy. Initially, the mucoadhesive performance of the films and wafers was assessed using a texture analyser to measure the stickiness, work of adhesion and cohesiveness as well as the effect of viscosity of simulated wound fluid [(2% w/w or 5% w/w bovine serum albumin)], 2% w/w mucin solution, drugs (streptomycin and diclofenac and glycerol (for films) on the adhesive properties of the composite films and wafers. The adhesion properties of the formulations have been further evaluated using ATR-FTIR spectroscopy to measure and compare the diffusion of mucin the two formulations to establish proof of concept for measuring mucin interaction with the films and wafers as indication of their adhesive performance. Here the bovine serum albumin and mucin were used as model proteins to simulate wound exudate and moist wound surfaces respectively.

2. Experimental

2.1 Materials and methods.

Bovine serum albumin, mucin from porcine stomach type three (bound sialic acid 0.5-1.5%), phosphate buffered saline tablet [(one tablet dissolved in 200 mL of deionized water yields 0.01 M phosphate buffer), 0.0027 M potassium chloride and 0.137 M sodium chloride, pH 7.4, at 25°C)], diclofenac sodium and streptomycin sulphate were all purchased from Sigma Aldrich, (Gillingham, UK). Glycerol, sodium alginate, tris(hydroxymethyl)aminomethane, calcium chloride dihydrate, gelatine, ethanol (laboratory grade) were all purchased from Fisher Scientific (Leicestershire, UK). Polyethylene oxide (Polyox™ WSR 301 ≈4000 kDa) was a gift from Colorcon Ltd (Dartford, UK), κ-carrageenan (Gelcarin GP 812 NF) was obtained from IMCD Ltd (Sutton, UK).

2.2 Preparation of films and wafers

2.2.1 Preparation of gels

The films and wafers were prepared as previously reported[8, 12] and summarised briefly below. Initially, blank aqueous polymer gels (70°C) of polyox (POL) with carrageenan (CAR)

(POL-CAR) and POL with sodium alginate (SA) (POL-SA) in weight ratios of POL/CAR 75/25 and POL/SA 50/50 respectively, with resultant overall concentration of 1% w/w (total polymer weight in gel), were prepared. The drug loaded gels were prepared by the addition of an ethanolic solution of diclofenac to the polymeric gel (as described above) at 70°C to obtain a final diclofenac concentration of 25% and 10% (w/w) for POL-CAR and POL-SA gels respectively. The gel was subsequently cooled to 40°C with constant stirring and an aqueous solution of streptomycin was added to achieve a final streptomycin concentration of 30 and 25% w/w for POL-CAR and POL-SA gels respectively. In the case of plasticised films, glycerol was added to the aqueous gels, to obtain a final concentration of 20% and 9% w/w for POL-CAR and POL-SA respectively for both the blank and drug loaded gels.

2.2.2 Preparation of films

The gels were poured into Petri dishes (diameter 90 mm) and dried in an oven at 40°C for 18 h, to obtain the films[8]. The dried films were carefully peeled off from the Petri dish, wrapped in parafilm® and kept in desiccators over silica gel at room temperature (18°C).

2.2.3 Preparation of wafers

To obtain the freeze-dried wafers, 10 gm of each homogeneous gel (no glycerol) was poured into separate 6 well moulds (diameter 35 mm) (Corning® CellBIND® Sigma Aldrich, Gillingham, UK). The gels were freeze-dried in a Virtis Advantage XL 70 freeze dryer (Biopharma Process Systems, Winchester, UK). The samples were initially cooled from room temperature to -5°C and then -50°C over a period of 10 h (at 200 mTorr) and then annealed at -25°C for 2 h before being frozen back to -50°C. The primary drying stage involved heating the samples in a series of thermal ramps to -25°C under vacuum (20-50 mTorr) for 24 h and secondary drying carried out at 20°C (10 mTorr) for 7 h[12].

The various formulations (films and wafers) prepared are summarised in Table 1.

2.3 Mucoadhesion studies by texture analysis (TA).

Adhesive measurements were performed on the different films and wafers (Table 1) using a TA.HD *plus* Texture Analyser (Stable Micro Systems, Surrey, UK) fitted with a 5 kg load cell. The films and wafers (n = 4) were attached to an adhesive probe (75 mm diameter) with the help of double sided adhesive tape using set gelatin gel as the mucosal substrate. The surface of the gelatin gel in a Petri dish (86 mm diameter), was equilibrated with 0.5 mL of simulated wound fluid [containing 2% or 5% bovine serum albumin , 0.02 M calcium chloride, 0.4 M sodium chloride, 0.08 M tris(hydroxymethyl) aminomethane in deionised water, pH 7.4±0.1][27] to mimic a wound surface.

Table 1: Optimised formulations used for the adhesion study. [(The 9% and 20% annotation represents the concentration (% w/w) of glycerol (GLY) present in the respective original POL-SA and POL-CAR gels used to prepare plasticised films)]. BLK and DL represent blank and drug loaded respectively.

Number	Formulation
1	POL-CAR-BLK-film
2	POL-CAR-DL-film
3	POL-CAR-BLK-20%GLY-film
4	POL-CAR-DL-20%GLY-film
5	POL-SA-BLK-film
6	POL-SA-DL-film
7	POL-SA-BLK-9%GLY-film
8	POL-SA-DL-9%GLY-film
9	POL-SA-BLK-wafer
10	POL-CAR-BLK-wafer
11	POL-SA-DL-wafer
12	POL-CAR-DL-wafer

Simulated wound fluid containing 2% w/w and 5% w/w bovine serum albumin represented thin and viscous exudate respectively. In addition, a separate gelatin gel was also equilibrated with 2% w/w solution of mucin (model protein) in PBS of pH 7.4 for direct comparison with the ATR-FTIR mucin diffusion experiment (described below). The probe, lined with film or wafer was set to approach the model wound surface with the following pre-set conditions: pre-test speed 0.5 mm/s; test speed 0.5 mm/s; post-test speed 1.0 mm/s; applied force 1 N; contact time 60.0 s; trigger type auto; trigger force 0.05 N and return distance of 10.0 mm. The adhesive strength (stickiness), total work of adhesion and cohesiveness were calculated using the *Texture Exponent 32*® software.
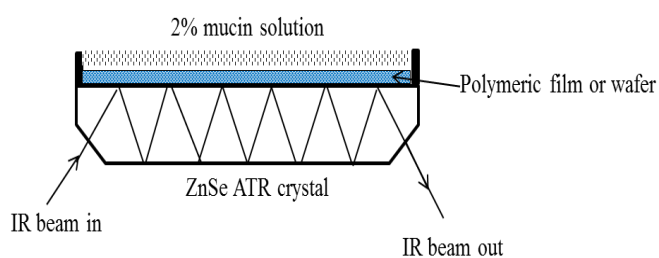
Figure 1: ATR assembly for *in situ* measurement of inter-diffusion of mucin solution through the films and wafers. This experimental set up is similar to that published previously[2].

2.4 Mucoadhesion studies by ATR-FTIR (diffusion of 2% w/w mucin).
A FTIR Nexus spectrometer (Thermonicolet, USA) equipped with an ATR accessory (Smart arc), KBR beam splitter and MCT/A detector having a cover to prevent spillage of mucin solution, was used for the diffusion studies as illustrated in figure 1. As shown in figure 1, the IR beam enters into the formulation to a small fixed depth and gets specifically attenuated according to the molecules present in this region.

The ATR crystal was ZnSe with dimensions of 50 mm long, 10 mm wide and 2 mm thick. Each formulation shown in table 1 was placed individually on the crystal and 0.5 mL of 2% w/w mucin solution (PBS 7.4 ± 0.1) was separately analysed. The wavenumber range was 4000-650cm^{-1}, mirror velocity of 1.8988, aperture 12, sample gain of 12 and spectra were collected every 9 sec with an average of 16 scans at resolution of 4 cm^{-1}. The final format obtained was in the form of absorbance with collection time of 12 mins. The spectrometer was linked to a computer equipped with *Omnic*® software which allows continuous automated collection of full spectra kinetically as a function of time.

2.4.1 Chemometrics
The data collected was analysed using chemometric multivariate data analysis. The chemometric analytical technique, employed in this study, was target factor analysis which is based on the numerical decomposition of a data matrix using the technique of factor analysis. Target factor analysis enables the deconvolution of fluid diffusion profiles through films and wafers using a targeted factor (mucin) in a complex data matrix without prior information of other overlapping unknown factors. This technique has been previously applied for the diffusion of solvents through membranes such as skin[28-29]. A schematic layout of the target factor analysis process is shown in supplementary section, Figure S1. The diffusion of 2% w/w mucin in PBS solution, was kinetically monitored through the various formulations (films and wafers) listed in table 1.

Target factor analysis was used to deconvolute the spectral profiles of the 2% w/w mucin solution together with those of the film and wafer formulations in the wavenumber range 1400-1700 cm^{-1}. The 1400-1700 cm^{-1} range was used because mucin has the amino group which can interact with polymers through hydrogen bond formation and used to follow the diffusion of mucin.[30] The relative rate of diffusion was then deduced from the data generated after subjecting to target factor analysis using *InSight*® software (InSight 2009, DiKnow Ltd, Rochester, UK) (see Figures S2 – S3 in the supplementary data section).

3. Results and discussion

3.1 Mucoadhesion studies by texture analysis [simulated wound fluid containing 2% and 5% w/w bovine serum albumin
Gelatin is obtained by controlled hydrolysis of collagens.. Its composition and biological properties are almost identical to its precursors and can therefore mimic a wound surface in the presence of simulated wound fluid[31]. A force of 1 N was applied due to the concern of newly formed tissue which may be interrupted or damaged if high forces were applied[32].

3.1.1 Unplasticised films. Figures 2 and 3 show the effect of viscosity of simulated wound fluid on the mucoadhesive

performance of the films. Both POL and CAR have strong hydrogen bonding groups while POL has sufficient chain flexibility and high molecular weight and viscosity which helps to improve the mucoadhesive performance of the prepared formulation[33]. When there is an intimate contact between the formulation and simulated wound fluid, hydrated polymer chains diffuse across the interface as a function of time. Mucoadhesion is mainly dependent upon the extent of diffusion and interfacial thickness between the two surfaces. With reference to mucoadhesion theories, various polymeric structures and functional groupings could have an effect on the degree of polymer-mucosal membrane interactions[13]. It is well accepted that mucoadhesive polymers such as POL, SA and CAR possess hydrophilic functional groups which are responsible for increased mucoadhesive performance [34].

Figure 2 shows the stickiness, work of adhesion and cohesiveness of POL-CAR and POL-SA films upon being detached from the model wound surface (gelatine) equilibrated with thin exudate. POL-SA-BLK films showed a stickiness (1.9±0.4 N) and work of adhesion (1.1±0.7 N.mm) values compared to those for POL-CAR-BLK films at (0.6±0.1 N) and (0.4±0.1 N.mm) respectively. The observed cohesiveness for both films was similar (POL-CAR-BLK 1.2±0.1 mm, POL-SA-BLK 1.3±0.2 mm). In the presence of viscous exudate, POL-CAR-BLK films showed higher values of stickiness (2.5±0.7 N) and work of adhesion (1.5±0.5 N.mm) which were decreased for POL-SA-BLK films (1.7±0.7 N and 1.1±0.5 N.mm respectively) (figure 3). This may be associated with the fact that the increased viscosity due to increased concentration of bovine serum albumin results in the formation of a gel like structure and helps more intimate contact with the substrate and therefore requires a stronger force to detach the POL-CAR-BLK films. In the presence of viscous exudate CAR gets hydrated to form a gel and is responsible for increased mucoadhesive performance. The increased intra-molecular attraction of the viscous exudate and the formation of internal cross-linkages on the gelatin surface might limit solvent diffusion into the polymeric matrix resulting in decreased mucoadhesion in the case of POL-SA-BLK film.

Various factors can influence mucoadhesive performance of formulations including structural constituents of polymers which affect degree of solvent diffusion and polymer chain entanglement. Roy and co-authors reported that hydrophilic polymers such as CAR and SA with anionic charges, exhibited high adhesion performance[35]. This is because such charged groups have an impact on the degree of hydration of the polymer when in contact with the mucosal surface[36]. In addition, polymer hydration and swelling polymer enhance the inter-diffusion process, allowing physical entanglement and increased surface availability for hydrogen bonding and electrostatic interaction between the polymer and the mucous network[36]. This might be the reason for the variation

in the mucoadhesive performance of films comprising two different polymers blended together in a single formulation.

3.1.2 Plasticised films. Figures 2 and 3 also illustrate the effect of plasticiser on the mucoadhesive performance of the films. In the presence of glycerol, mucoadhesive performance of the POL-SA-BLK films increased from 1.9±0.7 N to 2.4±0.3 N ($p<0.0233$) and increased from (0.6±0.1 N to 0.7±0.1 N) ($p = 0.1315$) for POL-CAR-BLK films. Glycerol acts as an adhesion promoter by enhancing hydrogen bonding between the polymeric chains and simulated wound fluid which is an important contributor to favourable adhesion performance for the POL-SA films. Another possible mechanism is that the plasticised films hydrate relatively more quickly in the presence of simulated wound fluid which consequently results in increased stickiness of the plasticised films. There was no significant difference ($p=0.75$) in the cohesiveness of POL-CAR-BLK (2.6±0.5mm) and POL-SA-BLK films (2.5±1.1mm).

The plasticised POL-CAR films (both blank and drug loaded) showed less detachment forces (stickiness). The presence of glycerol could possibly have interacted with CAR and POL a an increase in number and strength of hydrogen bonds between POL, CAR and glycerol could result in the formation of a strong network structure that resists the rapid penetration of water which might result in decreased mucoadhesive performance in the presence of thin exudate. In the presence of viscous simulated wound fluid (5% bovine serum albumin) the stickiness of blank POL-CAR-20%GLY (2.1±0.5N) was increased and POL-SA-9%GLY (1.7±0.8N)] was decreased whilst work of adhesion of BLK [POL-CAR-20%GLY (2.1±0.9 N) and POL-SA-9%GLY 1.1± 0.5N)] and cohesiveness [POL-CAR (3.4±0.4N) and POL-SA (2.8±1.0N)] was increased. This may be due to the fact that in the presence of glycerol, simulated wound fluid in higher concentration behaves as a slippery mucilage which results in reduced net mucoadhesive performance.

3.1.3 Drug loaded films. Further, figures 2 and 3 also depict the mucoadhesive performance of drug loaded (DL) films at different viscosities of simulated wound fluid. POL-CAR-DL films showed similar stickiness (0.8±0.1N) to the corresponding plasticized films (0.8±0.2N). A higher force was required to detach the POL-SA-DL films [(unplasticised 1.7±0.4N); (plasticised 1.9±0.4N),] when compared with the POL-CAR-DL films. Presence of drugs decreased the work of adhesion and cohesiveness for POL-SA and POL-CAR films with and without plasticizer. The observed work of adhesion for the POL-CAR-DL unplasticised and plasticised films were (0.5±0.1N.mm) and (0.4±0.1N.mm) respectively while it increased for POL-SA-DL unplasticised and plasticised films (1.0±0.4 and 1.0±0.5 N.mm) respectively but lower than the blank films. Interestingly, in the presence of viscous simulated wound fluid, stickiness increased for unplasticised (POL-CAR-DL) films (2.9±0.5N) and plasticised (POL-SA-DL-9%GLY) films (2.1±0.4N) but decreased for the plasticised [(POL-CAR-DL-

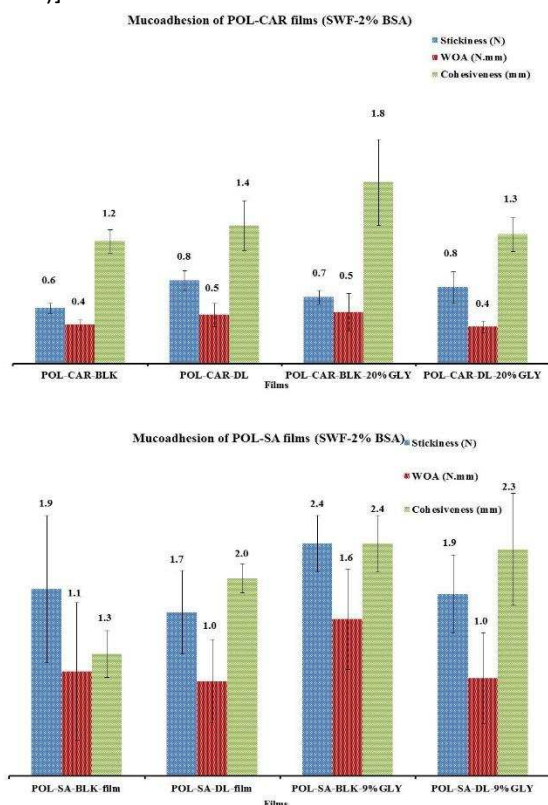20%GLY, 1.82±0.6N) and unplasticised (POL-SA-DL, 1.51±0.7N)] films.

Figure 2: Mucoadhesion profiles of POL-CAR and POL-SA films with simulated wound fluid (SWF) containing 2% w/w bovine serum albumin (BSA) showing effect of drug and glycerol on stickiness, work of adhesion (WOA) cohesiveness of the various films.

Figure 3: Mucoadhesion characteristics of POL-CAR and POL-SA films with SWF containing 5% w/w BSA.

The decrease in the work of adhesion in the presence of added drug can be attributed to two main reasons. Firstly, ionic interactions occurred between the anionic polymers (CAR and SA) and cationic streptomycin which had an effect on the hydrogen bonding mechanism between the polymers and simulated wound fluid which contains salts and proteins.

Secondly, Tobyn and co-workers reported that increased ionic strength of the media and the presence of sodium and potassium ions resulted in decreased adhesion[37]. Further, the sodium sulphate formed during gel preparation and ultimately present in the films further increased the ionic strength of the simulated wound fluid resulting in decreased adhesion. In the case of the films, the presence of sodium sulphate may have interfered with the physical properties of the delivery matrix and reduced the extent of adhesion to the gelatin substrate equilibrated with simulated wound fluid.

3.1.4 Freeze-dried wafers (BLK and DL). The effect of thin and viscous exudate on adhesive properties of POL-CAR and POL-SA wafers have previously been reported, with the POL-CAR-BLK and POL-SA-BLK wafers showing similar stickiness and cohesiveness values which decreased in the presence of drug
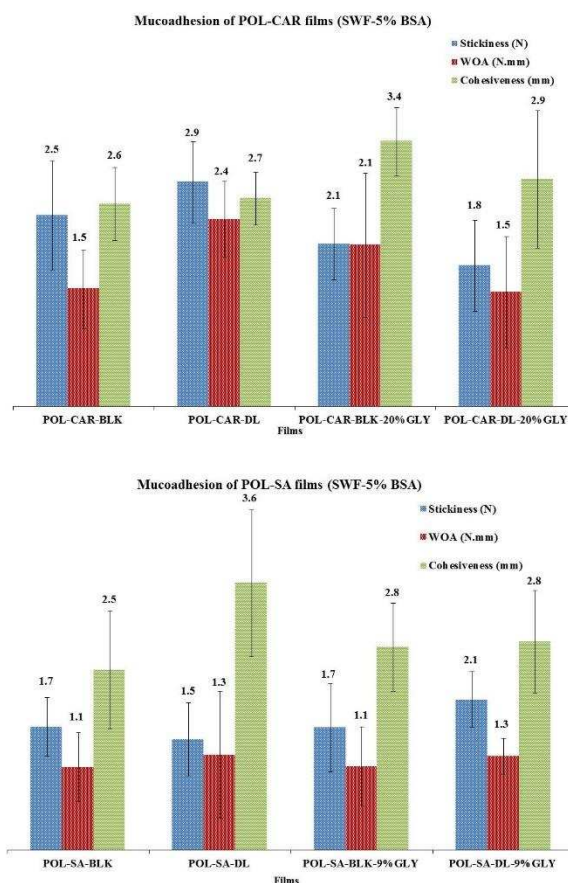
for thin simulated wound fluid[12]. This again may be because of the presence of sodium sulphate which has marked effect on the hydration of the wafers resulting in decreased stickiness.

Usually thin watery serous type exudate in a wound signifies possible bacterial infection, such as *Staphylococcus aureus* which produce staphylokinase, a known fibrinolytic, and degrades fibrin clots resulting in thin watery exudate[38-39]. The drug loaded POL-CAR and POL-SA wafers can help to manage such exudate due to their porous nature. Haemorrhagic and haemopurulent (viscous, sticky and thick) exudate signifies both infection and trauma and POL-CAR wafers can provide prolonged retention of wafers at the site of injury.

Overall, mucoadhesion results from wafers (both blank and drug loaded) confirmed that the porosity plays a critical role due to the ability to absorb simulated wound fluid and hydration of the polymeric network (POL, SA and CAR). The decreased stickiness in the drug loaded wafers was associated with the decreased porosity of these wafers due to the added drugs and subsequent salt (sodium sulphate) formation which inhibit rapid hydration of the wafers. From the results obtained it can be concluded that the wafers generally possessed good adhesive strength with the wound substrate

containing two different types of exudate compared to the films. Therefore these wafers can adhere to the wound site and protect the wound from the external environment with the absorption of large amounts of exudate, whilst maintaining their structure, which is a primary requirement for a formulation to function as an ideal wound dressing.

Overall, it appears that the POL-SA films and wafers can be used in the presence of normal exudate where concentration of protein is less to achieve prolonged retention time and bioavailability. POL-CAR films and wafers (POL-CAR and POL-SA) on the other hand can be used for wounds which produce viscous exudate to achieve better adhesive performance.
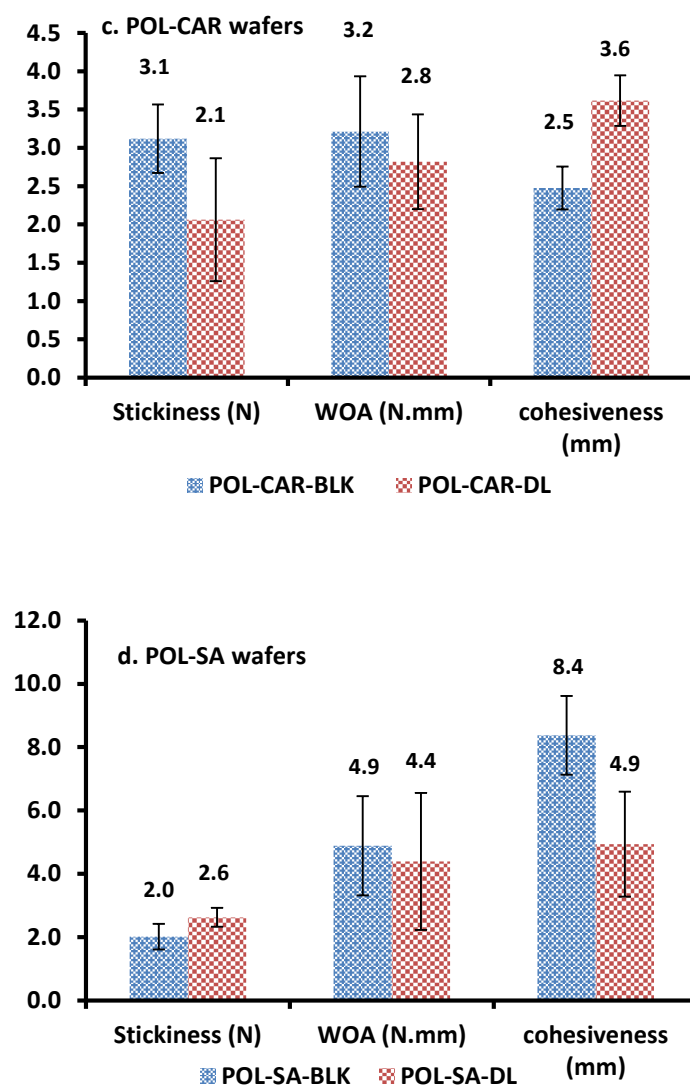
3.2 Mucoadhesion studies by texture analysis in the presence of 2% w/w mucin.

There are different theories proposed to explain the mucoadhesion process[13]. Mucoadhesive bond formation involves wetting and swelling of the polymer matrix, intimate contact between the substrate (mucin, simulated wound fluid, biological tissues) and polymer, as well as interpenetration and entanglement between polymer chains and the substrate[40]. For such mucoadhesion processes, diffusion of water and subsequent swelling behaviour of the mucoadhesive polymer based formulations has great impact on their adhesive performance. Sufficient amount of water is necessary to hydrate and expand the mucoadhesive network which exhibits available adhesive sites for bond formation and creates pores for diffusion of polymer chains to enhance the interpenetration[41]. The mucoadhesive performance of the films and wafers using 2% mucin solution by texture analysis are shown in figure 4. It was observed that the wafers had a higher mucoadhesion capacity compared to the films. Since wafers are porous in nature, they hydrate more quickly in the presence of mucin solution and form strong hydrogen bonding more quickly with the protein[42]. POL-CAR-BLK wafers showed the highest stickiness values (3.12±0.4 N) and lowest cohesiveness (2.48±0.3mm). The work of adhesion involved in the adhesion was decreased for the drug loaded wafers but was higher for the POL-SA films. As was the case with simulated wound fluid, the formation of sodium sulphate due to added drugs resisted the hydration of films which ultimately decreased the work of adhesion and also supports the swelling studies previously reported[9]. Strong hydrogen bonding and quick hydration was responsible for the increased work of adhesion of POL-SA wafers compared with POL-CAR wafers and ultimately increased the cohesiveness of the SA based wafers (POL-SA-BLK, 8.38±1.2 mm; POL-SA-DL 4.93±1.6 mm).

Addition of glycerol had a marked effect on the mucoadhesion performance of the films. Stickiness for the plasticised POL-CAR based films ranged from 2.05 to 2.21 N and from 1.91 to 2.37N for plasticised POL-SA based films. Overall, the adhesiveness for POL-SA based films was found in the

descending order of POL-SA-BLK-9%GLY > POL-SA-DL > POL-SA-DL-9%GLY > POL-SA-BLK. The adhesiveness for POL-CAR films was found in the decreasing order of POL-CAR-BLK-20%GLY > POL-CAR-DL-20%GLY > POL-CAR-BLK > POL-CAR-DL.

a. POL-CAR films

b. POL-SA films
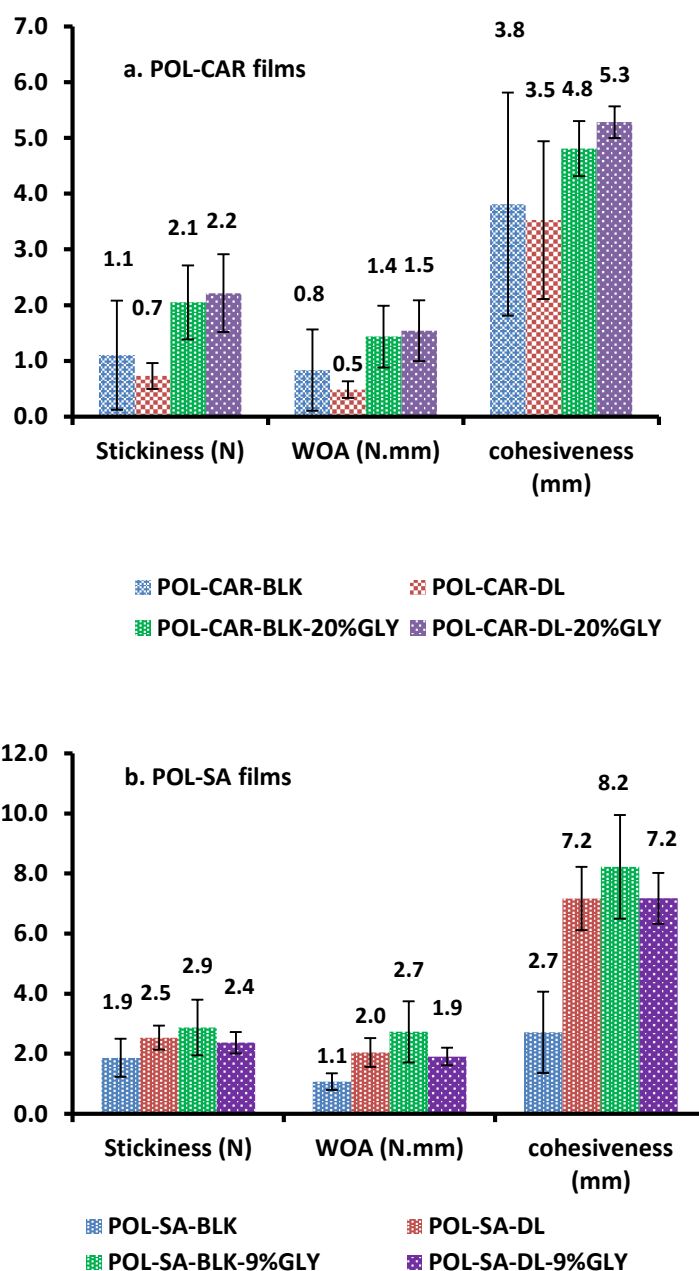
Figure 4: Mucoadhesion performance of films and wafers (POL-CAR and POL-SA) using texture analyser in the presence of 2% mucin solution showing stickiness, WOA and cohesiveness profiles.

3.3 ATR-FTIR analysis of mucin diffusion into films and wafers.

Figure 5 shows the ATR-FTIR spectra of mucin powder, mucin solution (2% w/w in PBS pH 7.4) and PBS only. There was a considerable difference between the IR spectra of mucin powder and mucin solution. Saiano *et al*.,[2] reported a band at 1550 cm^{-1} assigned to C=O stretching vibration of sialic acid of mucin type I-S from bovine submaxillary gland and a C=O stretching vibration at 1542 cm^{-1} for the mucin from porcine stomach type two, which has bound sialic acid from 0.5-1.5%. The IR spectrum of the mucin in PBS showed a strong amide I band at 1650 cm^{-1} whilst mucin powder showed amide I and amide II bands at 1650 cm^{-1} and 1550 cm^{-1} respectively, attributed to amino acids and oligosaccharides[43]. The IR spectral window of 1400-1700 cm^{-1} for mucin diffusion, where hydrogen bonding between amino group and polymer can be formed was chosen. This can provide helpful information of interpenetration of polymeric chains following diffusion of mucin solution diffusion and ultimately provides information on mucoadhesion.

In ATR-FTIR spectroscopy, wavelength of the incident radiation affects the depth of penetration of IR radiation into the sample. Time dependent spectral data from ATR-FTIR enabled detailed characterisation of the films and wafers. There were however, some challenging factors related to ATR-FTIR set-up that required careful consideration when analysing diffusion of mucin through the films and wafers. These included quality of contact of the formulations with the ATR crystal across the focal plane of the detector. This is important because absence of proper contact with the ATR crystal will produce inaccurate spectral profiles and can affect the diffusion results. Poor contact can be a function of the smoothness, porous (wafers) and thin (films) nature of the formulations[23].

McAuley reported that the wavelength influences the depth of penetration of IR radiation into the membrane[28]. This could therefore affect the interpretation of relative diffusion rates of the mucin dissolved in PBS when different windows of IR spectrum are analysed for the films and wafers. For that purpose, the spectrum window of 1400-1700 cm^{-1} was selected to evaluate the diffusion of mucin through the formulations, where peak of mucin is most prominent. There could be other factors that can interfere with the diffusion of mucin (due to spectral overlap) which could be avoided by using chemometric data analysis by selecting a particular reference spectral window of mucin. Chemometrics involves the extraction of information from chemical systems by data-driven means using methods frequently employed in core data-analytic disciplines such as multivariate statistics, applied mathematics, and computer science, in order to address problems in chemistry, biochemistry, medicine, biology and chemical engineering. Multivariate curve resolution techniques are particularly very efficient in the analysis and modelling of such data sets. The basic principle of multivariate curve resolution is based on the fact that each component in the multivariate spectral data contributes additively and linearly to the absorbance at each spectral wavenumber.

Table 2: Relative absorption values of the diffusion of mucin for the POL-CAR and POL-SA BLK and DL films and wafers.

| Formulations	Time (Sec)							
	50	100	200	300	400	500	600	700
POL-CAR-BLK-20%GLY	0.57±0.05	0.68±0.09	0.80±0.20	0.84±0.28	0.86±0.39	0.89±0.50	0.89±0.59	0.93±0.67
POL-CAR-BLK	0.24±0.05	0.28±0.06	0.47±0.07	0.75±0.08	0.84±0.12	0.94±0.20	0.92±0.28	0.94±0.35
POL-CAR-DL	0.05±0.05	0.20±0.07	0.39±0.14	0.62±0.24	0.72±0.37	0.82±0.49	0.91±0.90	0.98±1.03
POL-CAR-DL-20%GLY	0.66±0.14	0.28±0.35	0.09±0.55	0.18±0.52	0.32±0.65	0.42±0.76	0.57±0.84	0.75±0.99
POL-CAR-DL-wafer	0.34±0.09	0.21±0.17	0.16±0.28	0.42±0.31	0.68±0.33	0.81±0.35	0.72±0.43	0.87±0.51
POL-CAR-BLK-wafer	0.40±0.16	0.58±0.25	0.62±0.32	0.77±0.33	0.76±0.37	0.79±0.42	0.86±0.51	0.80±0.64
POL-SA-BLK-9%GLY	0.42±0.02	0.62±0.04	0.76±0.05	0.87±0.06	0.91±0.08	0.93±0.11	0.92±0.14	0.94±0.24
POL-SA-BLK	0.37±0.05	0.54±0.07	0.77±0.11	0.81±0.14	0.91±0.16	0.90±0.19	0.93±0.22	0.97±0.30
POL-SA-DL-wafer	0.05±0.04	0.25±0.07	0.65±0.12	0.72±0.15	0.86±0.19	0.75±0.23	0.80±0.31	0.86±0.43
POL-SA-DL-9%GLY	0.36±0.03	0.49±0.04	0.71±0.06	0.80±0.08	0.87±0.10	0.91±0.11	0.92±0.13	0.93±0.16
POL-SA-DL	0.35±0.03	0.50±0.04	0.70±0.07	0.79±0.09	0.88±0.11	0.91±0.13	0.95±0.15	0.97±0.19
POL-SA-BLK-wafer	0.30±0.10	0.50±0.12	0.68±0.17	0.64±0.25	0.81±0.32	0.70±0.40	0.86±0.46	0.82±0.66
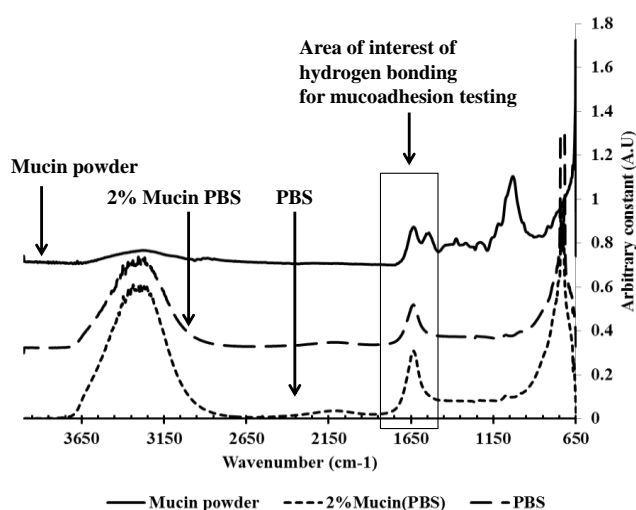
Figure 5: FTIR spectra of mucin powder, 2% mucin (dissolved in PBS) and PBS solution.

In addition, the observed absorbance is directly proportional to the concentration based on the Beer Lambert law. In the current study, the multivariate curve resolution technique used was based on target factor analysis and the theoretical details are discussed elsewhere[44-45]. The advantage of this approach is that models of real factors (here mucin peak at 1650cm^{-1} is considered as real factor which can form hydrogen bonds with polymeric films and wafers) can be systematically pieced together. This will ultimately give information about the mucoadhesion occurring between polymeric films and wafers). The profiles were normalised by setting the time frame of 780 s and a representative profile of three replicates are shown in figure 6. Such reproducibility measurements for the various samples was important given that the diffusion was measured over small distances as well as the combined effects of the many formulation variables (plasticiser, drugs, polymers, formed sodium sulphate and viscosity of simulated wound fluid) impacting on the mucoadhesive profiles being measured. The average of three profiles is shown on the same scale for comparison. As can be seen, though differences exist between the three replicates, the profiles were largely reproducible and shows the ability of the chemometrics approach combined with ATR-FTIR to measure the diffusion profiles of mucin through the films and wafers. In the figures plotted for the diffusion of mucin across the representative formulation, error bars were added for only positive values for clarity and comparison purposes as was the case in previous literature[2, 17].

Table 2 represents a summary of all the data from diffusion (relative intensity) of mucin across the various formulations used in the study. This data was used to study the effect of polymer, drug, and glycerol (only films) on the diffusion of mucin simultaneously monitoring the changes in the IR spectrum in the region of 1400-1700 cm^{-1}. The observed diffusion coefficient of mucin through the formulations are presented in table 3 below.

3.3.1 Diffusion profiles for POL-CAR and POL-SA films. Figures 7 and 8 show the normalised diffusion profiles for POL-CAR and POL-SA (blank and drug loaded) films obtained using the wavelength 1400-1700 cm^{-1}. Both POL-CAR-DL and POL-CAR-DL-20%GLY showed initial higher absorbance before 100sec possibly due to poor contact with the crystal which was reproducible for all the three replicates.
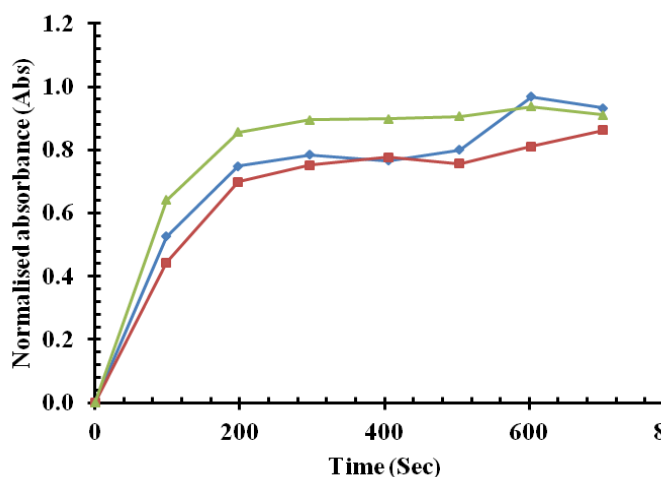
Figure 6: Representative normalised plots of the POL-SA-BLK films showing reproducibility (n = 3).

Table 3: Diffusion coefficient values for mucin through the optimised films and wafers.

| POL-CAR films /wafers	Diffusion coefficient "D" (cm^2/s)	POL-SA films/wafers	Diffusion coefficient "D" (cm^2/s)
POL-CAR-BLK	4.0×10^{-3}	POL-SA-BLK	6.2×10^{-3}
POL-CAR-DL	2.8×10^{-3}	POL-SA-DL	6.5×10^{-3}
POL-CAR-BLK-20%GLY	9.7×10^{-3}	POL-SA-BLK-9%GLY	7.4×10^{-3}
POL-CAR-DL-20%GLY	0.7×10^{-3}	POL-SA-DL-9%GLY	6.9×10^{-3}
POL-CAR-BLK-wafer	7.8×10^{-3}	POL-SA-BLK-wafer	6.1×10^{-3}
POL-CAR-DL-wafer	0.8×10^{-3}	POL-SA-DL-wafer	0.8×10^{-3}

Unplasticised POL-CAR-BLK films showed slower rate of diffusion of mucin through the films when compared to the plasticised films (Figure 9). The initial absorbance for unplasticised POL-CAR-BLK film was 0.24±0.05 which increased to 0.57±0.05 in the first 50 sec due to quicker diffusion of mucin solution through plasticised POL-CAR-BLK-20%GLY films. This may be due to the plasticizing effect of glycerol which has a higher affinity for water and increasing the mobility and elasticity of the films. Such a high water transfer inside the plasticised film matrix, has already been reported for glycerol plasticised CAR films[46]. POL-CAR-BLK films showed a steady increase in relative concentration and this is supported by the swelling studies previously reported[8]. Further, unplasticised POL-CAR-BLK films showed slower and steady diffusion of mucin which is due to the slow hydration of the POL and CAR to form a gel. After 400 sec, both plasticised and unplasticised POL-CAR films showed constant diffusion of mucin which may be associated with the saturation of mucin solution within the films and absorbance values ranged from 0.84 - 0.94.
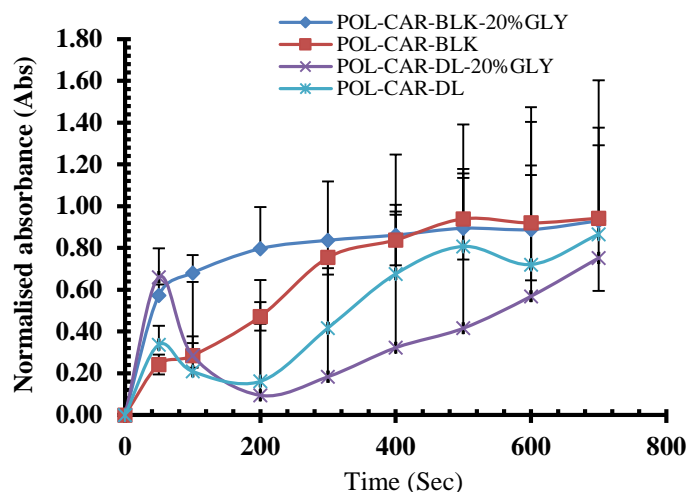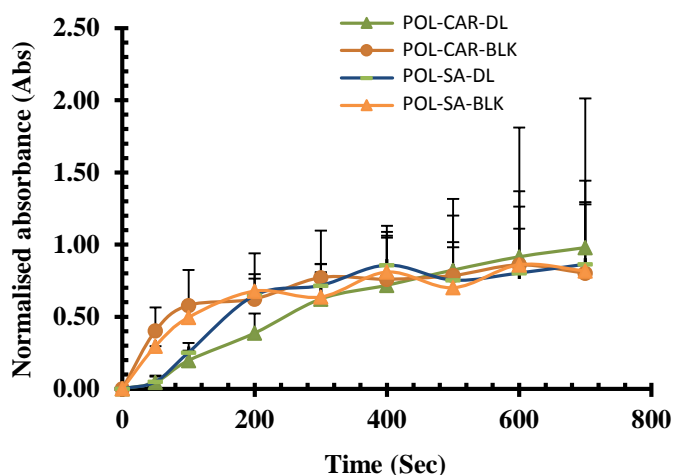

Figure 7: Normalised diffusion of mucin across POL-CAR films (mean ± SD, n=3)

All blank POL-SA films showed relatively faster swelling which ultimately increased diffusion of mucin through the BLK films when compared with the corresponding DL films. The individual profiles of mucin diffusion through the POL-SA films are shown in figure 8.
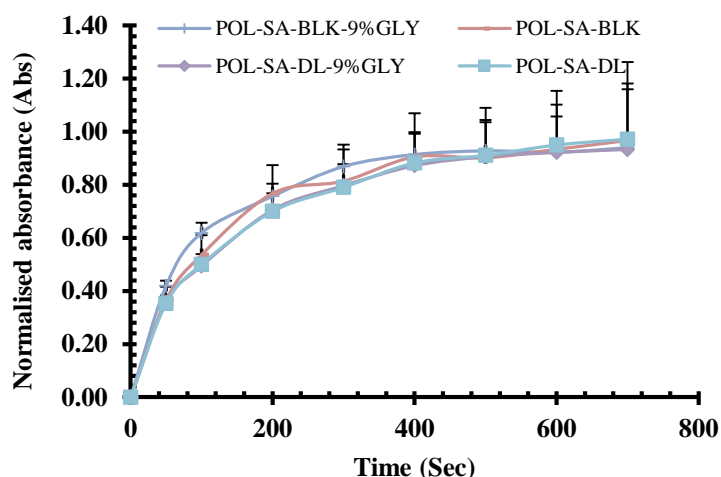
Figure 8: Normalised diffusion of mucin across POL-SA (BLK and DL) films (mean ± SD, n=3).

3.3.2 POL-CAR-BLK and POL-SA-BLK wafers. Figure 9 shows the individual profiles of mucin diffusion through the POL-CAR and POL-SA wafers. The diffusion of mucin was increased for the POL-SA-BLK wafers after 100 sec when compared with the POL-CAR-BLK wafers. This is associated with the swelling mechanism of the different polymers which supports the swelling studies previously reported[8].

Figure 9: Normalised diffusion of mucin across POL-SA (BLK and DL) wafers (mean ± SD, n=3).

3.3.3 Comparison of blank films and wafers. The diffusion profiles of the mucin through the blank films and wafers are compared in figure 10. Among the blank formulations, POL-CAR-BLK film showed slower diffusion of the mucin while the corresponding POL-CAR-BLK wafer showed a wavy diffusion profile which may be associated with the porous nature of the wafers which caused unequal distribution of mucin through these pore channels. Previously, Boateng and co-workers reported that wafers have the capacity to hydrate more quickly than their corresponding films[42]. The same trend was observed when comparing POL-SA-BLK film and wafer whilst diffusion was faster overall for both POL-SA-BLK films and wafers compared to their corresponding CAR containing formulations respectively. The quicker diffusion of the mucin through the POL-SA formulations is associated with the immediate swelling of the films and wafers and reported by Bajpai, and Sharma[47]. Such swelling in the matrix results in decreased absorbance which shows a plateau after 400 sec. As seen above, both films showed marked effect of glycerol which resulted in higher diffusion of mucin through these films. The overall trend observed for the diffusion of mucin through all blank formulations is associated with the glycerol (films) and swelling behaviour of individual polymers (POL, CAR and SA).

3.3.4 Comparison of drug loaded films and wafers. The overall diffusion of mucin through the drug loaded POL-SA films and wafers was higher compared to blank films and wafers and is shown in figure 11. As noted above, the added drug resulted in a decreased hydration capacity (due to formed sodium sulphate) which had overall impact on mucoadhesion properties. The same effect was observed for all drug loaded films and wafers which resulted in decreased diffusion of mucin through these formulations and supports the mucoadhesion studies by texture analysis.

The overall trend for the diffusion of mucin through the films and wafers as described above is summarised in table 3

below. This shows that in general, diffusion was faster through the POL-SA films than the corresponding POL-CAR films with the exception of blank plasticised films where the POL-CAR-BLK-20%GLY showed a higher diffusion than the POL-SA-BLK-9%GLY. This is due to the higher amounts of glycerol present in the POL-CAR films (20%GLY) compared to the POL-SA films (9%GLY).

3.4 Texture analysis versus ATR-FTIR spectroscopy. This study used two different techniques (texture analysis and ATR-FTIR spectroscopy) for the evaluation of the mucoadhesion properties of films and wafers. The former technique corresponds to the fracture, diffusion and wetting theories and relates the adhesive strength to the forces required for detachment of two interacting surfaces such as thin/viscous exudate and film or wafer after adhesion. Adamson[48] reported that the failure of adhesive bonds normally occurs at the weakest component which is typically cohesive failure within one of the adhering surfaces and it can be complicated to determine the weakest component in the current study due to blend of different polymers, plasticizer (in films) and different drugs. It is important to note that the adhesive strength depends upon the wetting phenomena of the polymer and relates to hydrophilicity of the polymer and excipients.
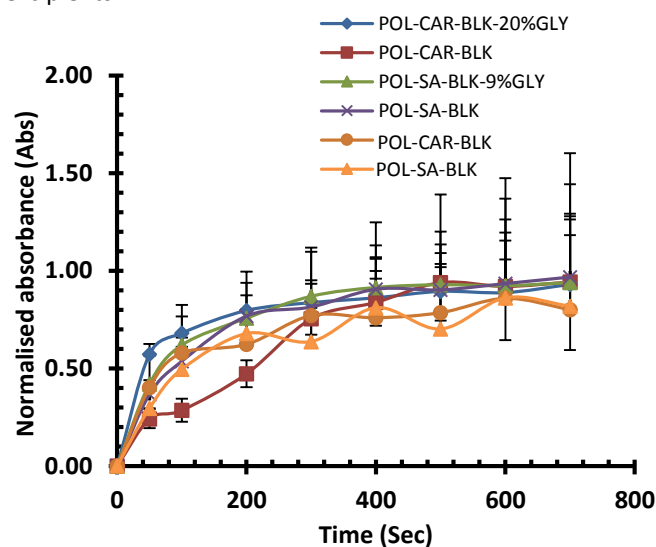
Figure 10: Normalised diffusion of mucin across BLK films and wafers (mean ± SD, n=3).

If the formulation has higher adhesional wetting, it results in higher mucoadhesion[47]. This trend was observed in the blank films and wafers which showed higher mucoadhesion compared to drug loaded films and wafers where wettability or hydration of the formulation was reduced due to the added drugs (sodium sulphate formed).
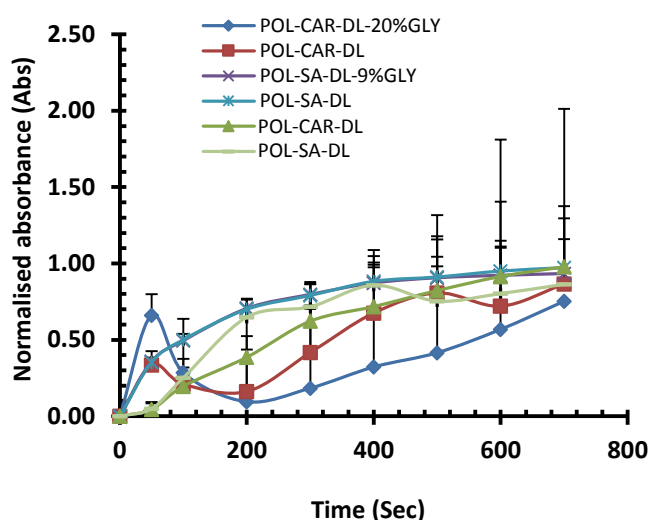
Figure 11: Normalised diffusion of mucin across DL films and wafers (mean ± SD, n=3).

The ATR-FTIR detection of diffusion of mucin on the other hand is based on the diffusion theory which represents inter-diffusion of polymer chains across an adhesive interface. It is driven by concentration gradients and affected by the available molecular chain lengths and their mobilities. The diffusion of mucin is dependent upon the diffusion coefficient and the time of contact. Smart reported that if the depth of penetration is sufficient, it creates a semi-permanent adhesive bond[13]. Another advantage of the FTIR approach is that unlike the texture analysis, the samples and target molecule can be directly analysed without the need for the gelatin mucosal substrate equilibrated with simulated fluid as well as need for a probe to ensure contact with the substrate followed by probe withdrawal. This introduce further steps to the measurement of mucoadhesive performance which can consequently introduce further variability.

Overall, the mucoadhesion data generated from these two techniques were therefore not directly comparable due to the different theories associated with these techniques. However, it gives an overview and proof of principle of precise parameters (such as effect of polymer, plasticizer and added drug) affecting the potential wound adhesion of films and wafer dressing.

Tamburic and Craig, in their study, compared three different methods (oscillatory rheometry, texture analysis in penetration mode and texture analysis in tensile detachment mode) to measure mucoadhesive performance of polymeric discs in the presence of mucin solutions[17]. The effect of different variables including neutralization states of the polymers, physical states of the formulation (hydrogel and compact discs) as well as mucin solution on mucoadhesive performance using the three *in vitro* approaches were

investigated. In the present study, we have compared the use of texture analyser and ATR-FTIR spectroscopy to determine mucoadhesive performance of solvent cast films and freeze-dried wafers in the present of simulated wound fluid (texture analyser) and mucin (ATR-FTIR). Though the techniques employed were different in both studies (except texture analyser), it is evident that such physico-mechanical analytical techniques are useful tools for predicting mucoadhesive performance. Each technique provides unique information relevant for explaining the many variables that impact on this important characteristic (mucoadhesion) essential for functional performance at mucosal and moist surfaces such as buccal mucosa and exuding wound surfaces.

Brako et al in a study similar to the current research, reported the relationship between viscosities (gel strengths) of polymer–mucin systems with mucoadhesion properties of polymers[49]. However, the authors used lower molecular weight of POL (200 KDa) to prepare nanofibers using pressured gyration, whereas in our study, films and wafers were prepared using high molecular weight POL combined with CAR or SA. They showed that POL on its own exhibited weaker interaction with mucin while blends of POL with carboxymethylcellulose demonstrated higher mucoadhesive properties. This is interesting as we have previously shown that blending of POL with either CAR or SA improved its functional performance (including swelling and adhesion) compared to POL on its own[8]. Further, whilst we employed texture analysis and ATR-FTIR combined with chemometrics to investigate adhesive performance as potential wound dressings, they employed a combination of texture analysis and atomic force microscopy to verify characterise their composite nanofibers for their mucoadhesive potential in vaginal applications. It is evident from both studies that employing more than one technique as well as composite formulations is an appropriate means of determining appropriate adhesive performance.

A number of characteristics, including polymer chain entanglement related to molecular weight[42] and net charge distribution, (cationic, neutral or anionic) have often been used to explain the mucoadhesive behaviour of polymers. In addition, several theories have been used to explain how mucoadhesion occurs. Two of these theories[13], the wetting theory including hydration also largely considered a prerequisite for facilitating hydrogen bonding for molecular interaction and the diffusion theory where interpenetration of polymer chains across an adhesive interface must have occurred prior to gel formation between the fibres and mucin (or exudate in the case of wound dressings).

4. Conclusions
Adhesive performance is critical as it determines the residence time of dressings at the wound site to allow for sustained drug release and eventual bioavailability. In the texture analysis study, the main factors affecting adhesive

performance were polymers, glycerol, viscosity of simulated wound fluid and the presence of drugs. Overall, the adhesiveness for POL-SA based films was found in the descending order of POL-SA-BLK-9%GLY > POL-SA-DL > POL-SA-DL-9%GLY > POL-SA-BLK. The adhesiveness for POL-CAR films was found in the decreasing order of POL-CAR-BLK-20%GLY > POL-CAR-DL-20%GLY > POL-CAR-BLK > POL-CAR-DL. ATR-FTIR spectroscopy combined with chemometrics (target factor analysis) showed that mucin diffused independently through the solvent and across the films and wafers. POL-CAR films showed slower diffusion when compared with POL-SA films whilst POL-CAR wafers showed higher diffusion than the POL-SA wafers which decreased in the presence of drug. Plasticized films (POL-CAR and POL-SA) showed higher diffusion of mucin than the blank and drug loaded films. Finally, the results show a proof of principle of specific formulation parameters such as polymer, plasticizer and added drug affecting the potential wound adhesion of films and wafer dressings.

6. Notes

‡ **Supplementary data**: Please see appendix below.

7. References

1   O. Sarheed, B.K. Rasool, E. Abu-Gharbieh and U.S. Aziz. *AAPS PharmSciTech*, 2014, **16(3)**, 601-609.
2   F. Saiano, G. Pitarresi, G. Cavallaro, M. Licciardi and G. Giammona, *Polymer,* 2002, **43(23)**, 6281-6286.
3   S. Baljit and P. Lok. *Journal of Mechanical Behaviour of Biomedical Materials*, 2012, **9**, 9-21.
4   J.S. Boateng and O. Catanzano. *Journal of Pharmaceutical Sciences*. 2015, *DOI 10.1002/jps.24610*.
5   T.J. Sill and H.A. von Recum, *Biomaterials*, 2008, **29**, 1989–2006.
6   P. Sofokleous, E. Stride, W. Bonfield and M. Edirisinghe. *Materials Science and Engineering C*, 2013, **33**, 213–223.
7   S. Zhang, B. T. Karaca, S.K. VanOosten, E. Yuca, S. Mahalingam, M. Edirisinghe and C. Tamerler. *Macromolecular Rapid Communications.* 2015, **36**, 1322–1328.
8   H.V. Pawar, J. Tetteh and J. Boateng, *Colloids and surfaces. B, Biointerfaces,* 2013, **102**, 102-10.
9   J.S. Boateng, H.V. Pawar and J. Tetteh, *International Journal of Pharmaceutics,* 2013, **441(1–2)**, 181-191.
10 N. Thirawong, J. Nunthanid, S. Puttipipatkhachorn and P. Sriamornsak, *European Journal of Pharmaceutics and Biopharmaceutics,* 2007, **67(1)**, 132-140.
11 N.A. Peppas and P.A. Buri, *Journal of Controlled Release,* 1985, **2**, 257-276.
12 H.V. Pawar, J.S. Boateng, I. Ayensu and J. Tetteh, *Journal of Pharmaceutical Sciences,* 2014, **103(6)**, 1720 - 1733.
13 J.D. Smart, *Advanced Drug Delivery and Reviews*. 2005, **57**, 1556-1568.
14 D. Ameye, D. Mus, P. Foreman and J.P. Remon. *International Journal of Pharmaceutics*, **301(1-2)**, 170 – 180.
15 H.H. Alur, S.I. Pather, A.K. Mitra and T.P Johnston. *International Journal of Pharmaceutics*, **188(1)**, 1 – 10.
    .
16 S. Tamburic and D.Q.M. Craig, *European Journal of Pharmaceutics and Biopharmaceutics*, 1997, **44(2)**, 159-167.
17 E. Jabbari, N. Wisniewski and N.A. Peppas, *Journal of Controlled Release,* 1993, **27(1)**, 89-89.
18 J.O. Morales and J.T. McConville, *European Journal of Pharmaceutics and Biopharmaceutics,* 2011, **77(2)**, 187-199.
19 N.A. Peppas and J.J. Sahlin, *International Journal of Pharmaceutics,* 1989, **57(2)**, 169-172.
20 J.S Boateng, R.B. Amador, O. Okeke and H.V. Pawar, *International Journal of Biological Macromolecules*. 2015, **79**, 63 – 71.
21 A.M. Avachat, K.N. Gujar and K.V. Wagh. *Carbohydrate Polymers*, 2013, **91(2),** 537-542.
22 R.R. Shiledar, A.A. Tagalpallewar and C.R. Kokare. *Carbohydrate Polymers*, 2014, **101**, 1234-1242.
23 J. Tetteh, K.T. Mader, J.M. Andanson, W.J. McAuley, M.E. Lane, J. Hadgraft, S.G. Kazarian and J.C. Mitchell, *Analytica Chimica Acta,* 2009, **642(1-2)**, 246-256.
24 J. Gabrielsson, N.O. Lindberg, and T. Lundstedt, *Journal of Chemometrics,* 2002, **16(3)**, 141-160.
25 E.K. Malinowski, Factor analysis in chemistry. Second eds., Wiley-interscience publication, John Wiley and Sons. Inc, New Jersey, 1991.
26 S. Wold, M. Sjostrom and L. Eriksson, *Chemometrics and Intelligent Laboratory Systems,* 2001, **58(2)**, 109-130.
27 S. Lindsay, M. Del-Bono, R. Stevenson, S. Stephens and C. Breda, Symposium on Advanced Wound Care (SAWC), 2010. Florida, USA (poster).
28 W.J. McAuley, K.T. Mader, J. Tetteh, M.E. Lane and J. Hadgraft, *European Journal of Pharmaceutical Sciences,* 2009, **38(4)**, 378-383.
29 M. Dias, J. Hadgraft, S.L. Raghavan and J. Tetteh, *Journal of Pharmaceutical Sciences,* 2004, **93(1)**, 186-196.
30 M.M. Patel, J.D. Smart, T.G. Nevell, R.J. Ewen, P.J. Eaton and J. Tsibouklis, *Biomacromolecules*, 2003, **4(5)**, 1184-1190.
31 V. Rattanaruengsrikul, N. Pimpha and P. Supaphol, *Macromolecular Bioscience,* 2009, **9(10)**, 1004-1015.
32 F. Momoh, J.S. Boateng, S.C. Richardson, J.C. Mitchell, B.Z. Chowdhry, *International Journal of Biological Macromolecules,* 2015, **81**, 137–150.
33 H. Boyapally, R.K. Nukala, P. Bhujbal and D. Douroumis, *Colloids and Surfaces B-Biointerfaces,* 2010, **77(2)**, 227-233.
34 S. Lefnaoui and N.Moulai-Mostefa, *Starch-Starke,* 2011, **63(8)**, 512-521.
35 S. Roy, K. Pal, A. Anis, K. Pramanik and B. Prabhakar, *Designed Monomers and Polymers,* 2009, **12(6)**, 483-495.
36 J. M. Gu, J.R. Robinson and S.H.S. Leung, *Critical Reviews in Therapeutic Drug Carrier Systems,* 1988, **5(1)**, 21-67.
37 M.J. Tobyn, J.R. Johnson and P.W. Dettmar, *European Journal of Pharmaceutics and Biopharmaceutics,* 1997, **43(1)**, 65-71.
38 R. White and K.F. Cutting, *World Wide Wounds*, 2006, **1**, *1-5*.
39 M.H. Braff, A.L. Jones, S.J. Skerrett and C.E. Rubens, *Journal of Infectious Diseases,* 2007, **195(9)**, 1365-1372.
40 P. Sriamornsak, N. Wattanakorn, J. Nunthanid and S. Puttipipatkhachorn, *Carbohydrate Polymers,* 2008, **74(3)**, 458-467.
41 S.H.S. Leung and J.R. Robinson, *Journal of controlled release*, 1990, **12(3)**, 187-194.
42 J.S. Boateng, A.D. Auffret, K.H. Matthews, M.J. Humphrey, H.N.E. Stevens and G.M. Eccleston, *International Journal of Pharmaceutics,* 2010, **389(1–2)**, 24-31.
43 M, Khajehpour, J.L. Dashnau and JM. Vanderkooi, *Analytical Biochemistry*, 2006, **348**, 40-48.
44 E.K. Malinowski, Factor Analysis in Chemistry. Second eds., Wiley-Interscience, John Wiley and sons. Inc, New Jersey, 1991.
45 P.J. Gemperline, Practical Guide to Chemometrics, Second Edn. Taylor and Francis Group, LLC, 2006.
46 T. Karbowiak, H. Hervet, L. Léger, D. Champion, F. Debeaufort and A. Voilley, *Biomacromolecules,* 2006, **7(6)**, 2011-2019.
47 S.K. Bajpai and S. Sharma, *Reactive Functional Polymers,* 2004, **59**, 129–140.

48 A.W. Adamson, Physical Chemistry of Surfaces, Wiley-Interscience, New York, 1990, 110–113.

49 F. Brako, B. Raimi-Abraham, S. Mahalingam, D.Q.M. Craig and M Edirisinghe, *European Polymer Journal,* 2015, **70**, 186–196.

8. APPENDIX: SUPPLEMENTARY DATA[‡]
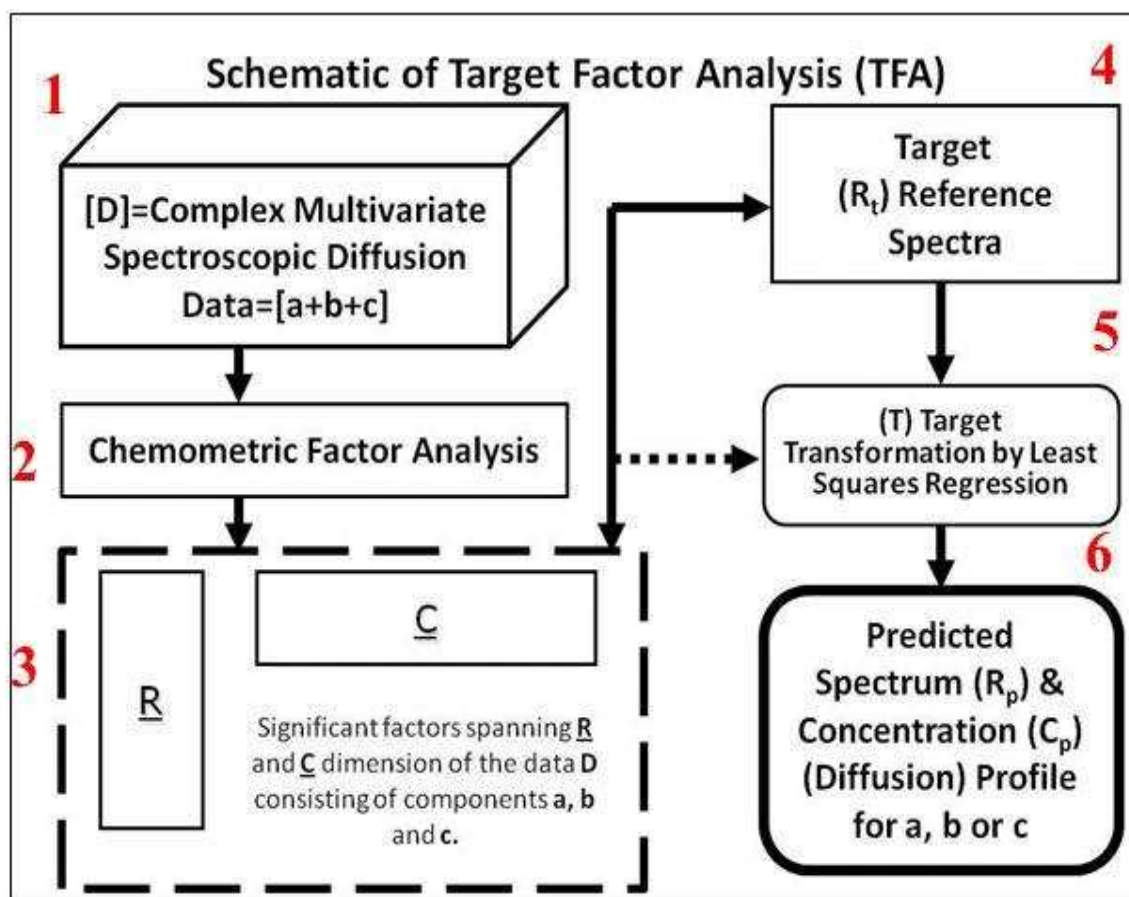
Figure S1: Schematic layout of the target factor analysis process: (1) complex data matrix (D); (2) chemometric factor analysis; (3) significant factors affecting data matrix; (4) target reference spectra (Rt) used in combination with the R and C; (5) target transformation through least square regression; (6) predicted spectrum (Rp) and concentration profile (Cp).

A typical data analysis using 2% mucin on POL-CAR-BLK in the wavenumber window 1400-1700cm^{-1}, with a spectral correlation minimum limit of 0.8, is shown below. Figures S2a and S2b show a typical data set obtained from the ATR-FTIR setup equivalent to data matrix D in the schematic figure S1 (box 1). The data was subjected to chemometric factor analysis to obtain the significant factors in row domain R and corresponding column domain C as shown in S1 (box 2). These significant factors for the diffusion of 2% mucin through POL-CAR-BLK film are shown in figure S2 c, d and e. The significant factors were estimated using various methods such as factor indicator function (Figure S2c), the percentage significant level (Figure S2d) and the cumulative percentage variance (Figure S2e) to determine true factor space. Detailed background on the determination of the significant factors is described elsewhere (Malinowski, 1991). Figure S3 shows the deconvoluted diffusion output of the 2% mucin through the POL-CAR-BLK film and other factors within the same spectra window used for the analysis. It is clear that besides mucin (e.g. in figure S1 box 6), two other factors (e.g. b and c in figure S1 (box 6) also contributed to the diffusion process. These hidden profiles would be very difficult to know without the use of multivariate target factor analysis. The diffusion profile obtained in figure S3 (b) enabled the relative diffusion coefficient to be calculated by determining the slope of the curve before the film or wafer was saturated (i.e. before the plateau of the curve). The process described above was used to analyse all other formulations to deduce the diffusion profiles for the mucin and thus enable direct comparison of the relative rate of diffusion between the different formulations by normalisation of data.

Journal Name

ARTICLE
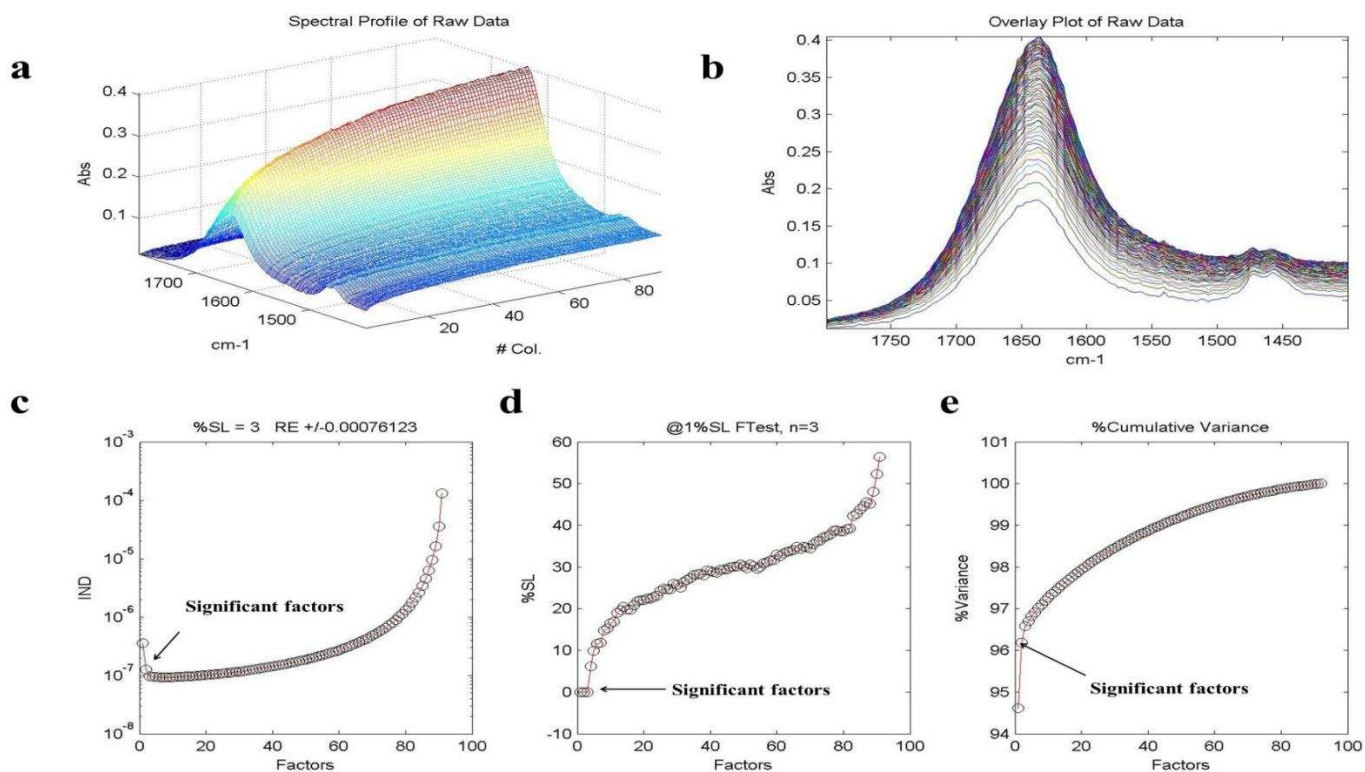
Figure S2: (a) shows a typical ATR-FTIR 3D spectral profile for the selected window 1400-1700 cm^{-1} (b) overlay plot of raw ATR-FTIR spectral profile (c) significant factor calculated using factor indicator function (IND) (d) percentage significant level (%SL) plotted against the number of factors (e) cumulative percentage variance (CPV) accounted for the abstract factor reproduction. The arrow indicates the cut off point for the selection of number of significant factors.
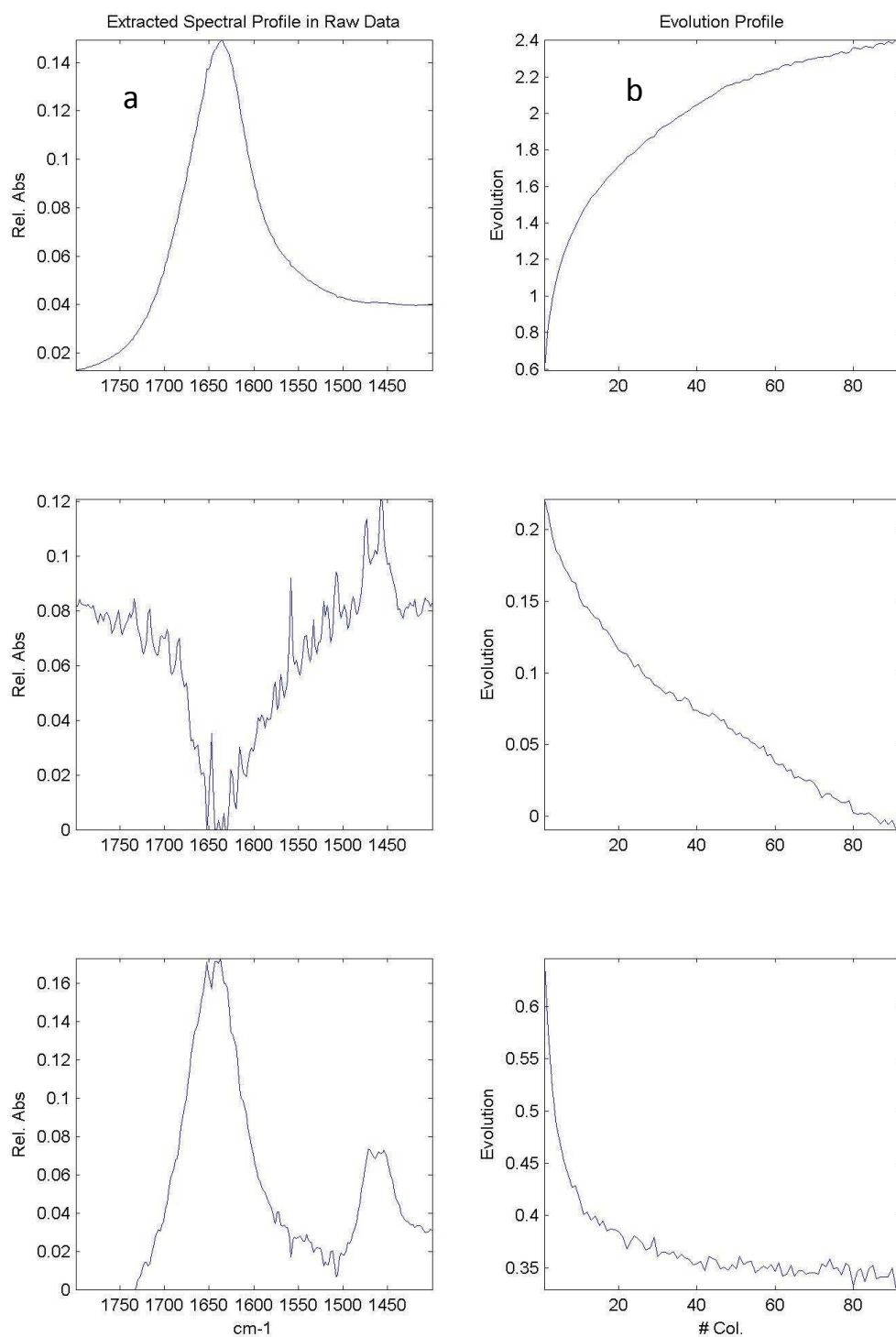
Figure S3: The deconvoluted diffusion output of the 2% mucin and other factors within the spectrum window 1400-1700cm^{-1} used for the analysis.